

Article

Supplementary Materials for Molecular Mechanisms of Protein-Lipid Interactions and Protein Folding of Heterogeneous Amylin and Tau Oligomers on Lipid Nanodomains that Link to Alzheimer's

Natalia Santos ¹, Luthary Segura ¹, Amber Lewis ¹, Thuong Pham ² and Kwan H. Cheng ^{1,2,*}

¹ Neuroscience Department., Trinity University. San Antonio, TX 78212, USA; nsantos@trinity.edu (N.S.); lsegura1@trinity.edu (L.S.); alewis2@trinity.edu (A.L.)

² Physics Department, Trinity University, San Antonio, TX 78212, USA; tpham3@trinity.edu (T.P.)

* Correspondence: kcheng1@trinity.edu; Tel.: (+1-210-999-8469)

Table of Contents

- Figure S1. Modeling of homogeneous oligomers.
- Figure S2. Minimum distance analysis of 1tam binding to the raft membrane.
- Figure S3. Minimum distance analysis of 2tam binding to the raft membrane.
- Figure S4. Mindist heatmaps of 1tam/raft complexes.
- Figure S5. Mindist heatmaps of 2tam/raft complexes.
- Figure S6. Compositions of annular lipids of membrane-bound oligomers.
- Figure S7. Phospholipid order disruptions by hetero- and homo-amylin oligomers.
- Figure S8. Protein structures of membrane-bound homo-amylin and -tau oligomers.
- Figure S9. Contact maps of membrane-bound 1tam and 2tam.

Videos S1-S4 are published in Mendeley Data.

Cheng, Kwan (2023), "Hetero-oligomers in solution and binding to the raft membrane", Mendeley Data, V1, doi: 10.17632/8vb23c48ph.1

<https://data.mendeley.com/datasets/8vb23c48ph/1>

- Video S1. Creation of 1tam in solution
(0 to 5 μ s; 0.1 μ s/frame; filename: Video 1.gif)
- Video S2. Creation of 2tam in solution
(0 to 5 μ s; 0.1 μ s/frame; filename: Video 2.gif)
- Video S3. Lateral view of 1tam binding to raft membrane.
(0-15 μ s; 0.1 μ s/frame; filename: Video 3.gif)
- Video S4. Transverse view of 1tam binding to raft membrane.
(0-15 μ s; 0.1 μ s/frame; filename: Video 4.gif)

Multiscale modeling of homogeneous amylin and tau oligomers

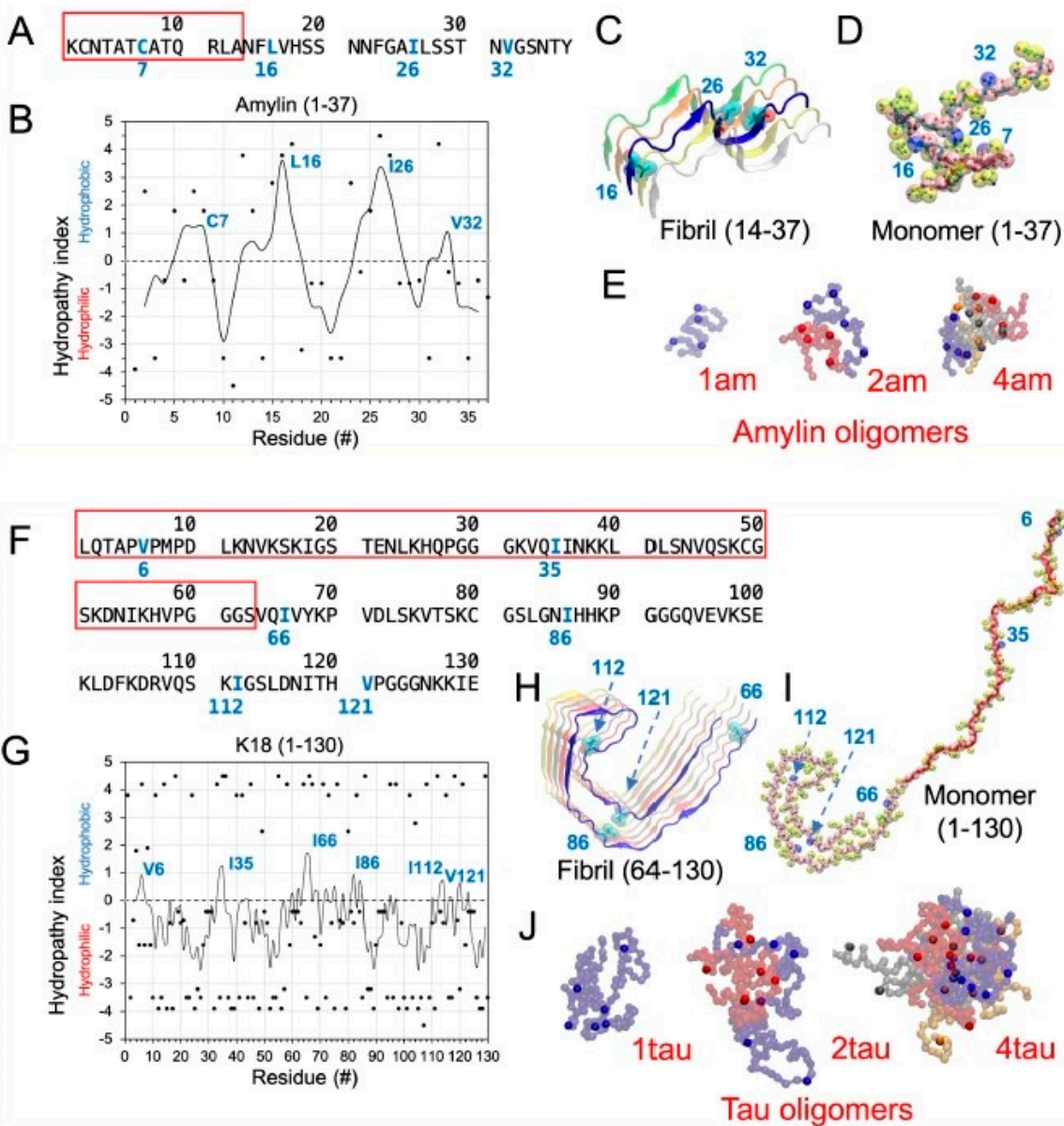
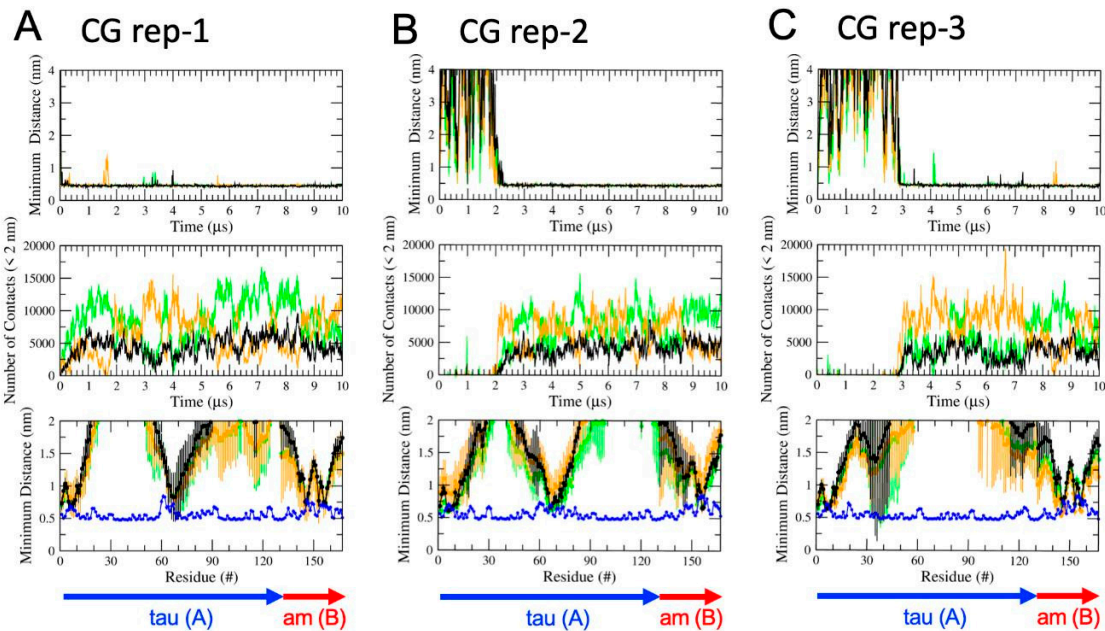


Figure S1. Modeling of homogeneous oligomers. The primary sequences of amylin (A) and tau-K18 or tau (F), and the corresponding hydrophobicity plots (B, G) are shown. The initial AA structure of a 37-residue-long amylin or 130-residue-long tau monomer was created by extracting a chain from the CryoEM fibril structure (PDB: 6VW2 or 5O3L) and attaching a 13- or 63-residue-long coil to its N-terminus (C, D) or (H, I), respectively. After an AA-to-CG transformation followed by a 5- μ s-long-CG simulation, 1am (E) or 1tau (J) monomer in solution was created. By placing multiple monomers in different locations of a simulation box, amylin (E) or tau (J) oligomers were created via self-aggregation. All CG simulations were performed under physiological conditions of 0.1 M NaCl, 1 atmospheric pressure, and 310 K. The protein structures are shown in backbone ribbon with chain A in blue, chain B in red, chain C in gray, and chain D in orange. The major hydrophobic residues of amylin and tau as depicted by the hydrophobicity plots are shown in brighter beads.

Mindist 3-panel analysis of CG 1tam/raft complexes



Mindist 3-panel analysis of AA 1tam/raft complexes

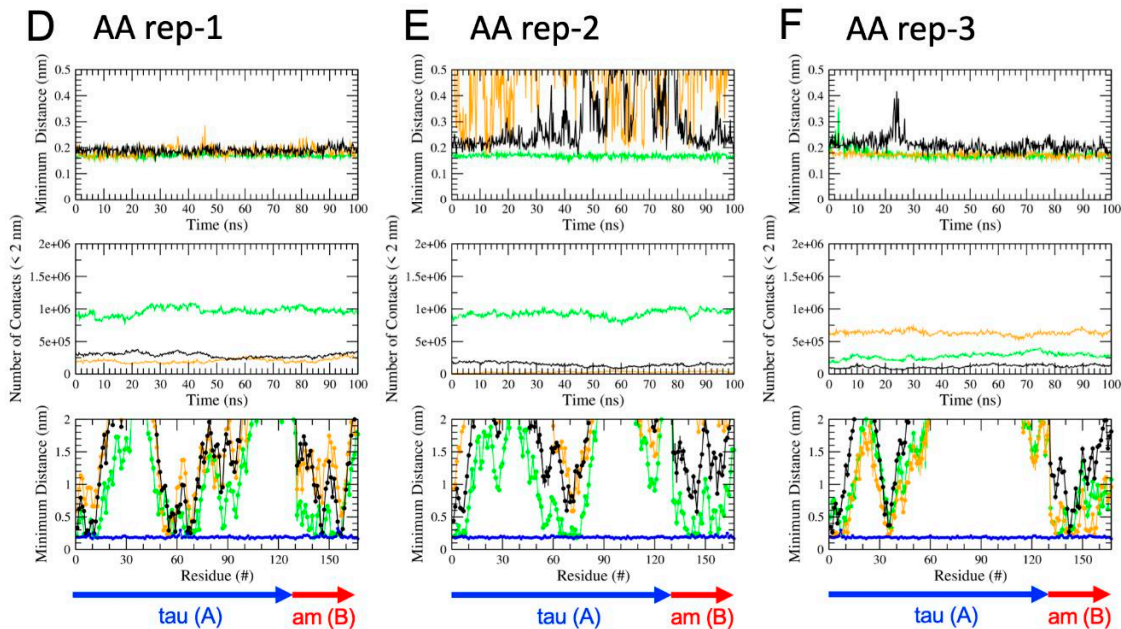
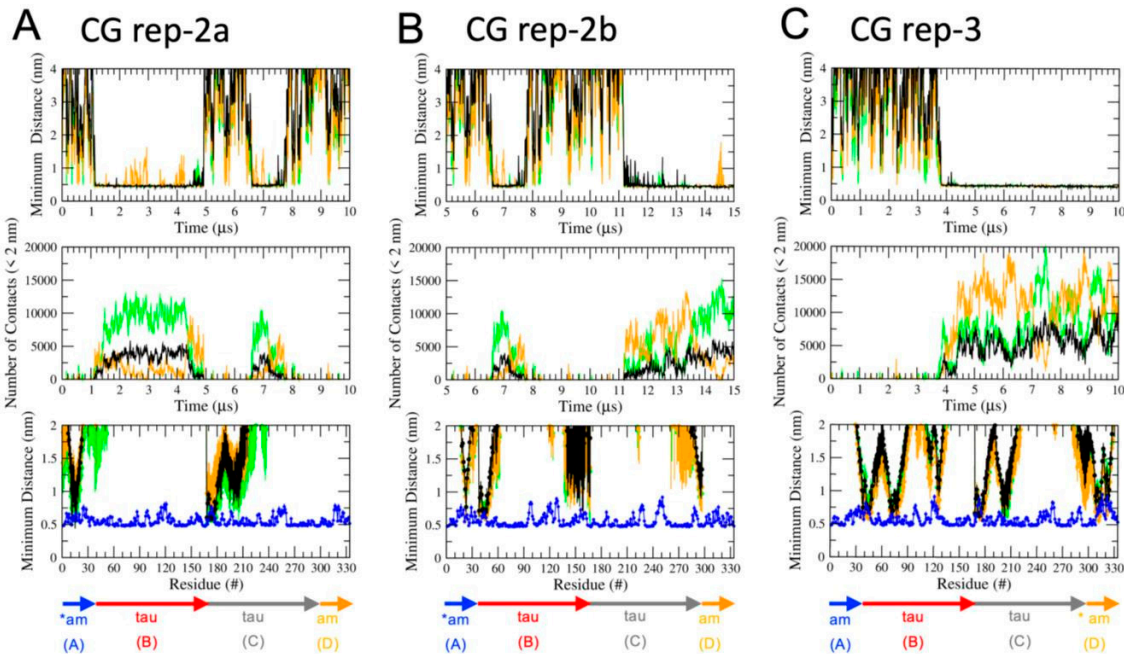


Figure S2. Minimum distance analysis of 1tam binding to the raft membrane. Three-panel plots of the minimum distance (*mindist*) between protein lipid (or water) atoms (*mindist*) of three replicates, rep-1, rep2, and rep-3, of the 1tam/raft complex in CG (A-C) and AA (D-F) simulations are shown. Each initial structure of the AA simulation was obtained from the 10 μ s CG structure after a CG-to-AA transformation of each replicate. The upper panel shows the *mindist* between protein and lipid atoms vs. time, the middle panel shows the number of contacts within 2 nm between protein and lipid atoms vs. time. The lower panel shows the time-averaged *mindist* between protein and lipid (or water) atoms vs. residue # over the last 5 μ s for CG and the last 50 ns for AA. All *mindist* values are color coded based on the lipid types, DPPC in green, DLPC in orange, CHOL in black, and water in blue. The error bar represents the standard deviation of the mean. The protein residue locations of the tau and amylin (am) chains inside the 1tam are identified by the blue (chain A) and red (chain B) arrows, respectively.

Mindist 3-panel analysis of CG 2tam/raft complexes



Mindist 3-panel analysis of AA 2tam/raft complexes

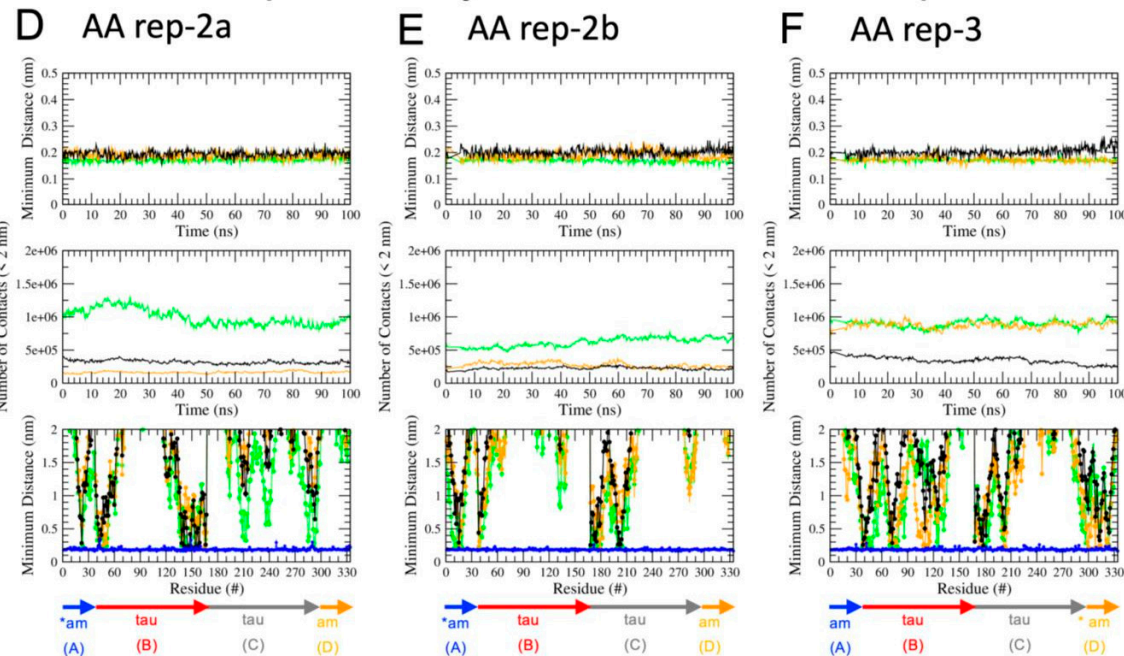


Figure S3. Minimum distance analysis of 2tam binding to the raft membrane. Three-panel plots of the minimum distance (*mindist*) between protein lipid (or water) atoms (*mindist*) of three replicates, rep-2a, rep-2b, and rep3, of the 2tam/raft complex in CG (A-C) and AA (D-F) simulations are shown. Note that rep-2a and rep-2b were from a single 15 μ s-long CG simulation showing stable membrane binding within the intervals of 1.1–4.8 and 11.2–15 μ s. The initial structure of the AA simulation was obtained from the equilibrated 4.8, 15, or 10 μ s CG structure after a CG-to-AA spatial transformation of rep-2a, rep-2b, or rep-3, respectively. The upper panel shows the *mindist* between protein and lipid atoms vs. time, the middle panel shows the number of contacts within 2 nm between protein and lipid atoms vs. time. The lower panel shows the time-averaged *mindist* between protein and lipid (or water) atoms vs. residue # over 1.1 to 4.8 in rep-2a, 11.2–15 in rep-2b, or 5–10 μ s in rep-3 for the CG and the last 50 ns in all replicates for AA. The protein residue locations of the tau and amylin (am) chains inside the 2tam are identified by the blue, red, gray, and orange arrows, corresponding to chains A (am), B (tau), C (tau), and D (am), respectively.

Mindist heatmaps of 1tam/raft complexes

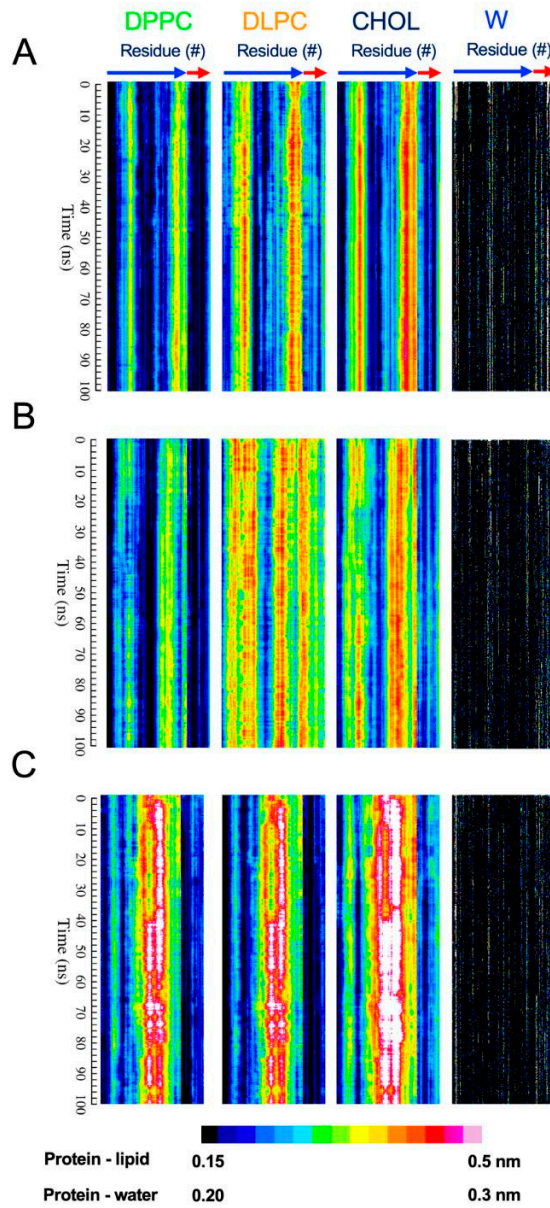


Figure S4. *Mindist* heatmaps of 1tam/raft complexes. Plots of color-coded minimum distance (*mindist*) between protein and lipid (or water) of 1tam/raft complexes vs. protein chain residue (*x*-axis) and simulation time (*y*-axis) are presented in a 3D heatmap format for rep-1 (A), rep-2 (B), and rep-3 (C). The protein residue locations of the tau and amylin (am) chains inside the 1tam are identified by the blue (chain A) and red (chain B) arrows, respectively.

Mindist heatmaps of 2tam/raft complexes

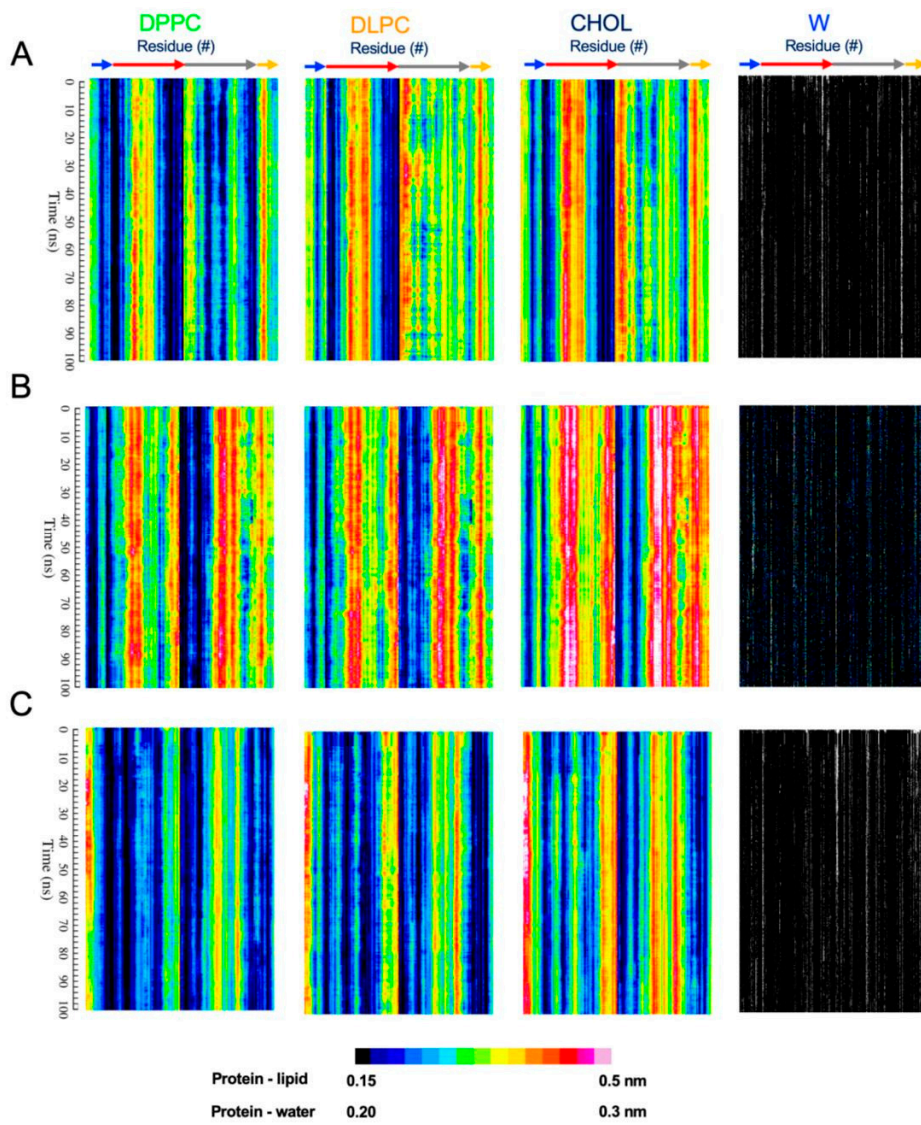


Figure S5. *Mindist* heatmaps of 2tam/raft complexes. Plots of color-coded minimum distance (*mindist*) between protein and lipid (or water) of 2tam/raft complexes vs. protein chain residue (*x*-axis) and simulation time (*y*-axis) are presented in a 3D heatmap format for rep-1 (A), rep-2 (B), and rep- (C). The protein residue locations of the tau and amylin (am) chains inside the 2tam are identified by the blue, red, gray, and orange arrows, corresponding to chains A (am), B (tau), C (tau), and D (am), respectively.

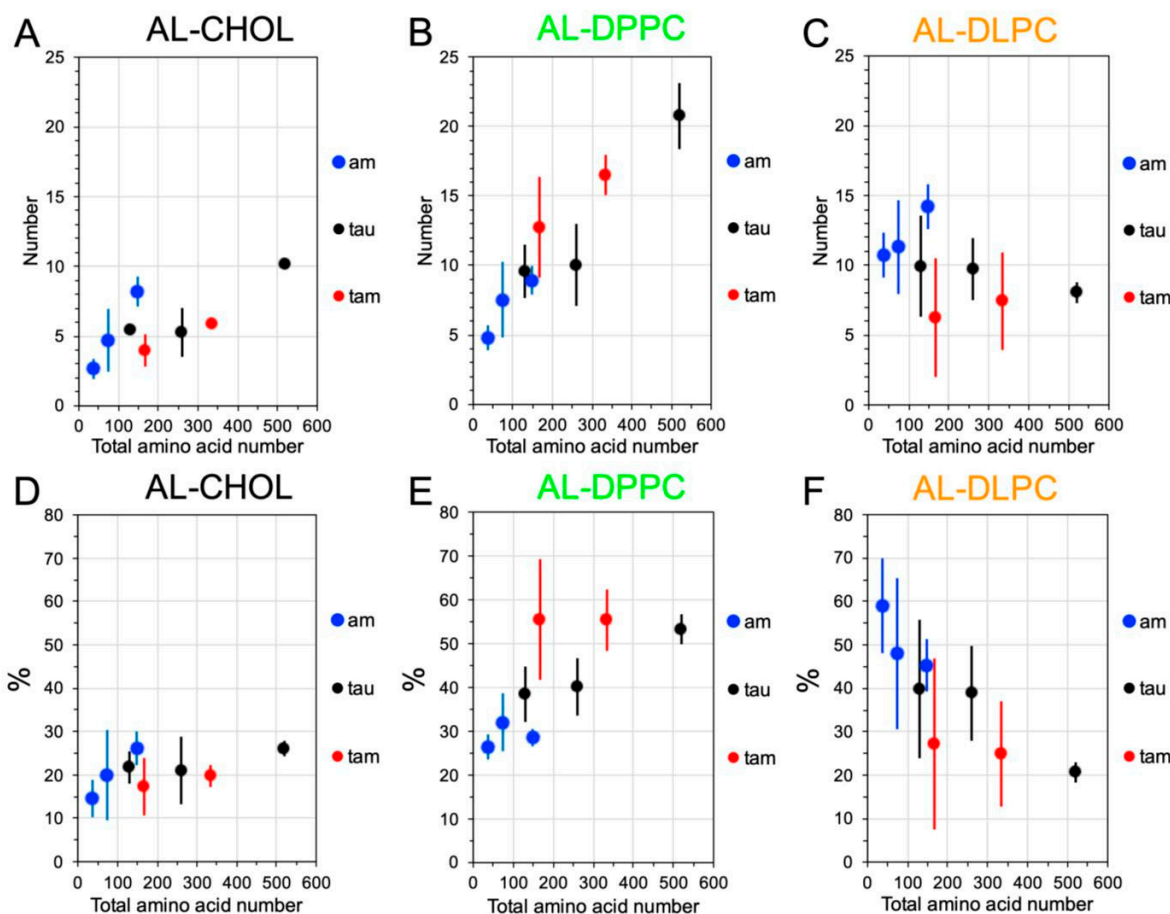


Figure S6. Compositions of annular lipids of membrane-bound oligomers. The total numbers (A-C) and percentages (D-E) of CHOL (A, D), DPPC (B, E), and DLPC (C, F) in the 0-0.5 nm annular lipid (AL) shells of homo-amylin (blue) and -tau (black) oligomers and hetero-oligomers (red) are given. The oligomers are sorted according to their total amino acid numbers. Each data point represents the time- and replicate-averaged value over the last 50 ns of AA simulations and across all replicates. The oligomers are placed in the plots according to their total amino acid numbers. The error bars are standard errors of the means.

Phospholipid order disruption effects of heterogeneous tau-amylin and homogeneous amylin oligomers

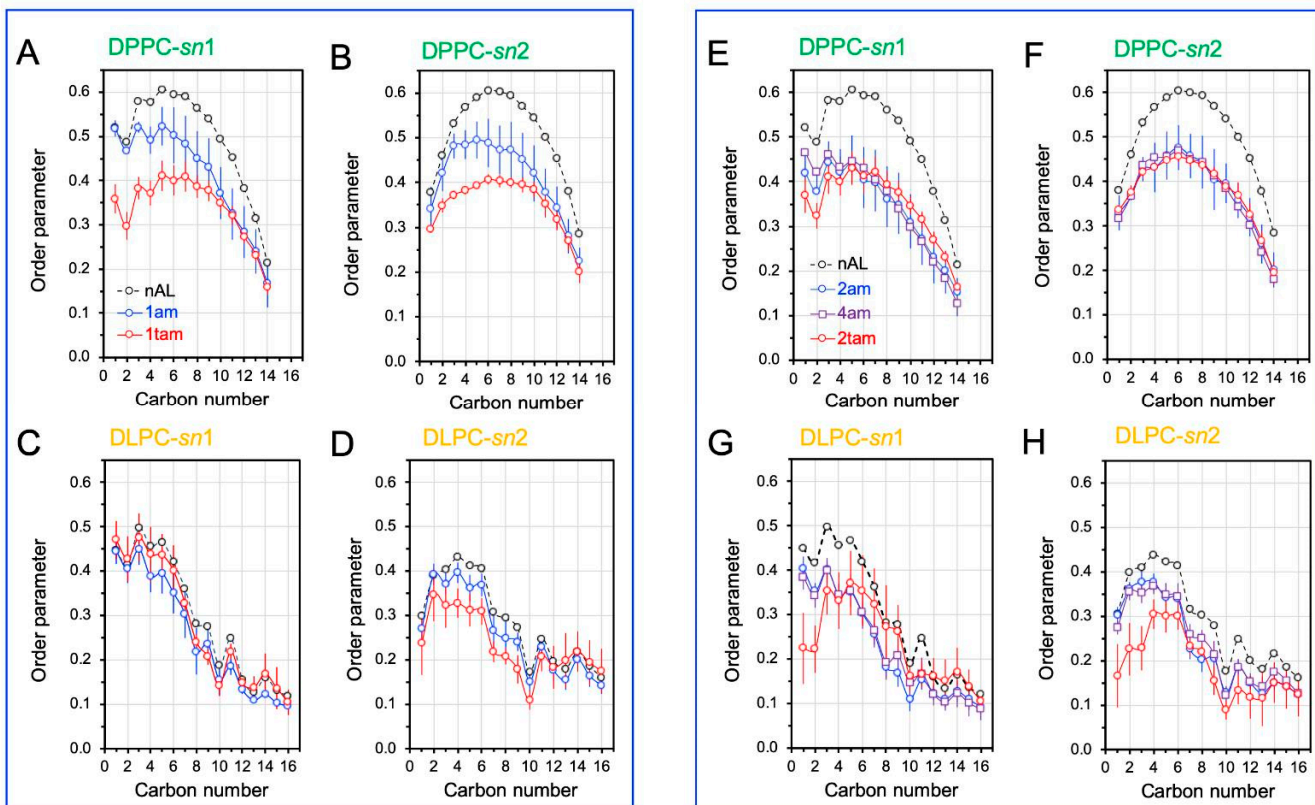


Figure S7. Phospholipid order disruptions by hetero- and homo-amylin oligomers. The time- and replicate-averaged plots of the phospholipid orientational order parameter vs. lipid acyl chain carbon number, or order profiles, over the last 50 ns of the AA simulation and across all replicates, for DPPC (A-F) and DLPC (C-H) in the 0-0.5 nm annular lipid (AL) shells of the hetero-oligomers (1tam and 2tam) and homo-amylin oligomers (1am, 2am, and 4am) are shown. The lipid profiles of the lipids outside the AL shell, or non-annular lipids (nAL), are also shown as controls. The data points for the sn-1 (A, C, E, G) and sn-2 (B, D, F, H) chains are presented. The error bar indicates standard error of the mean for each data point.

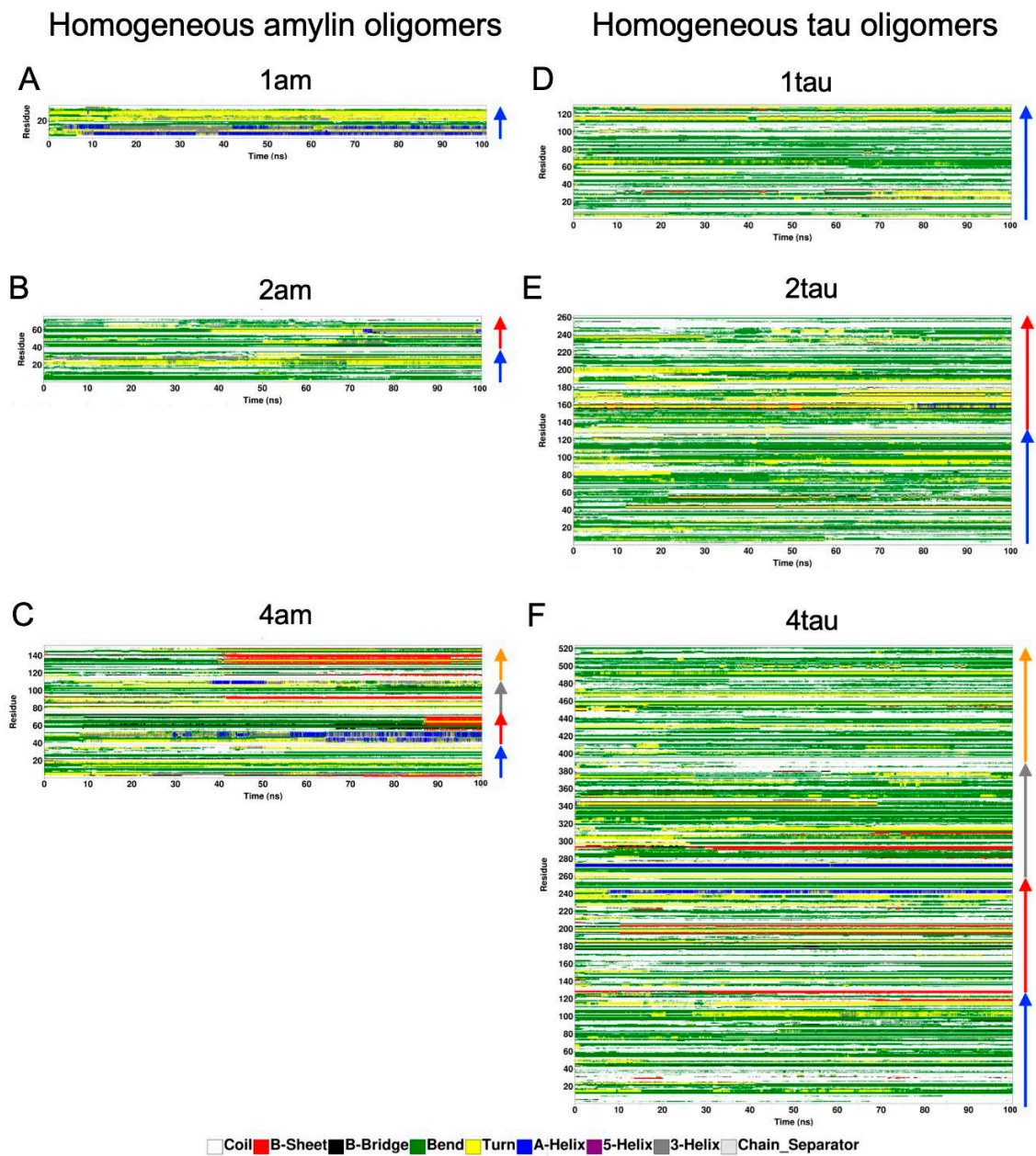


Figure S8. Protein structures of membrane-bound homo-amylin and -tau oligomers. The secondary structure plots show the membrane-bound homo-amylin (A-C) and -tau (D-F) oligomers in a DSSP format in which the color-coded secondary structure of each residue (y-axis) was calculated as a function of simulation (x-axis). The protein residue locations of the amylin or amylin chains are identified by the blue (chain A), red (chain B), gray (chain C), and orange (chain D) arrows, respectively.

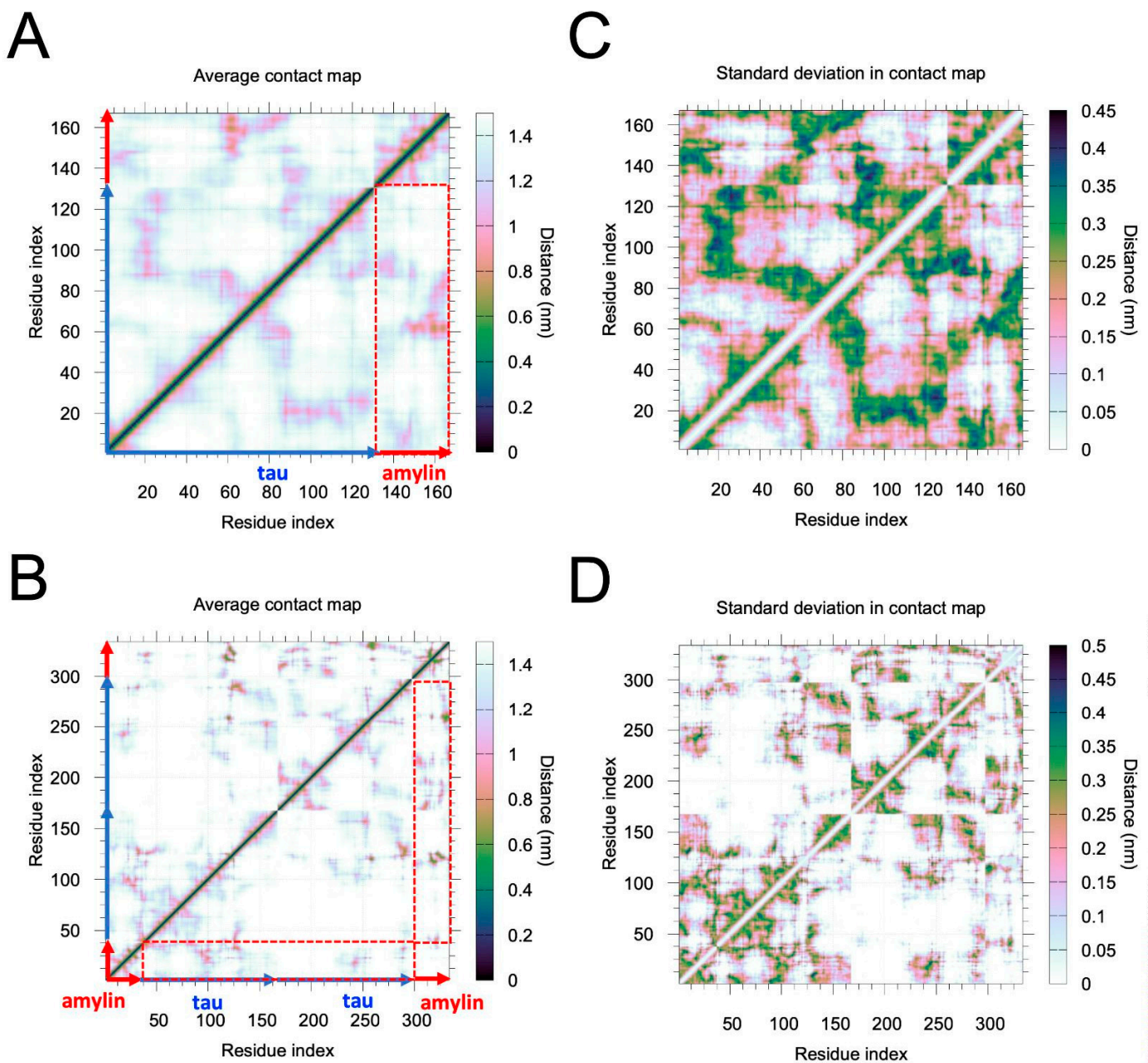


Figure S9. Contact maps of membrane-bound hetero-oligomers. The average (**A, B**) and the standard deviation (**C, D**) of contact between each amino acid residue in a hetero-dimer (**A, C**) and hetero-tetramer (**B, D**) on the raft membrane are shown. The contact regions between the residues of amylin (red arrow) and those of tau (blue arrow) are identified in dashed rectangles in the average contact maps. The color-coded data points represent the average and standard deviation of contact between each amino acid residue in the oligomer from the last 5 μ s of the CG simulation.